Secondary Structure and Topology of Human Interleukin 4 in Solution†

Christina Redfield,‡ Lorna J. Smith,‡ Jonathan Boyd,‡ G. Mark P. Lawrence,§ Robert G. Edwards,§ Richard A. G. Smith,§ and Christopher M. Dobson*,‡

Inorganic Chemistry Laboratory and Department of Biochemistry, University of Oxford, South Parks Road, Oxford OX1 3QR, England, and SmithKline Beecham Pharmaceuticals, Yew Tree Bottom Road, Great Burgh, Epsom, Surrey KT18 5XQ, England

Received July 22, 1991

ABSTRACT: Human interleukin 4 (IL-4) has been studied by 2D and 3D NMR techniques using uniformly ^{15}N-labeled recombinant protein. Assignment of resonances for all but 3 of the 130 residues of the recombinant protein has been achieved, enabling the secondary structure of the protein to be defined. This consists of four major α-helical regions and one short section of double-stranded antiparallel β-sheet. Analysis of distance and angle restraints derived from NMR experiments has enabled the overall molecular topology to be determined. This is related to that found for other four-helix proteins but has several distinctive features including cross-linking of helices by means of three disulfide bonds and a short section of β-sheet. The structural analysis gives support to the hypothesis that many helical cytokines have a common fold and provides a basis for understanding the biological function of IL-4.

Human interleukin 4 (IL-4[1] or B-cell stimulatory factor) is a pleiotropic cytokine that acts as a growth factor for T and B lymphocytes and stimulates activated B lymphocytes to express the low-affinity IgE receptor and to switch to the secretion of IgE (Howard et al., 1982; DeFrance et al., 1987a,b; Vercelli et al., 1989). IL-4 itself has potential pharmaceutical properties, for example in the cytokine therapy of cancer (Kawakami et al., 1988). To begin the process of understanding the biological activities of IL-4, and particularly its receptor binding properties, at a molecular level, three-dimensional structural information is required. As yet no X-ray structure is available for IL-4, although preliminary studies have shown that the molecule forms well-ordered crystals that diffract to beyond 2.8-Å resolution and so are suitable for detailed diffraction analysis (Cook et al., 1991). In addition, CD studies of the protein in solution have shown that it has a high percentage of α-helical structure and has a high stability over a wide range of solvent conditions (Windsor et al., 1991).

NMR spectroscopy is a powerful technique that can now be used to give detailed descriptions of protein structures (Wüthrich, 1989). As NMR provides the structure of proteins in solution, the method complements the use of X-ray diffraction for the determination of protein structures. In this paper we describe NMR studies designed to investigate the structure of IL-4 in solution. IL-4 has 129 residues and a molecular weight of nearly 15000 in its nonglycosylated form. Although it has proved possible to assign and interpret NMR spectra of proteins of this size using 2D ^1H NMR [e.g., Redfield and Dobson (1988)], the procedure is complicated by spectral overlap and chemical shift degeneracies. Recent developments in NMR methodology have shown that the complexity of the task can be reduced substantially by the use of 3D NMR techniques and a ^{15}N-enriched protein sample (Marion et al., 1989; Driscoll et al., 1990; Clore & Gronenborn, 1991) as in these experiments the spectral resolution is greatly improved by the extension into a third dimension. This strategy was therefore adopted in the present study. Analysis of the assigned 3D experiments has enabled the secondary structure and overall fold of the protein to be identified. The results indicate that the structure is based on a four-helix bundle motif and provide some details of its topology.

Materials and Methods

IL-4 Preparation and ^{15}N Labeling. Recombinant human IL-4 was expressed using a synthetic gene in bacterial (*Escherichia coli*) cells. The recombinant protein differs from native human IL-4 by the addition of an N-terminal methionine residue, referred to in this work as residue "0", and the absence of carbohydrate. The recombinant protein was found to have activity similar to that of reference preparations of IL-4 using T-cell proliferation and other assays. Refolding and purification were carried out using modifications of published procedures (van Kimmenade et al., 1988). The ^{15}N-labeled protein was obtained from growth of *E. coli* on a minimal medium incorporating ^{15}N-labeled $(NH_4)_2SO_4$ as the sole nitrogen source. All the 3D NMR experiments were performed on a sample of 2 mM protein at pH 5.3 and 35 °C; for the hydrogen-exchange experiments the pH was reduced to 4.5 and the temperature to 20 °C.

NMR Spectroscopy. All the NMR experiments were performed on a home-built spectrometer, using GE/Nicolet software and digital control equipment, which operates at 500.1 MHz for ^1H and 50.7 MHz for ^{15}N and uses a Bruker reverse probe head. The sequential assignments were carried out using experimental data from three separate ^1H–^{15}N 3D experiments: a ^1H–^{15}N 3D NOESY–HMQC experiment (Messerle et al., 1989), a ^1H–^{15}N 3D HOHAHA–HSQC experiment incorporating a WALTZ-16 spin-lock period (Driscoll et al.,

† Contribution from the Oxford Centre for Molecular Sciences which is supported by the U.K. Science and Engineering Research Council and the Medical Research Council.

* To whom correspondence should be addressed.
‡ University of Oxford.
§ SmithKline Beecham Pharmaceuticals.

[1] Abbreviations: IL-4, interleukin 4; Ig, immunoglobulin; CD, circular dichroism; NMR, nuclear magnetic resonance; NOE, nuclear Overhauser enhancement; HOHAHA, homonuclear Hartmann–Hahn spectroscopy; NOESY, nuclear Overhauser enhancement spectroscopy; COSY, *J*-correlated spectroscopy; HSQC, heteronuclear single-quantum coherence; HMQC, heteronuclear multiple-quantum coherence; RMSD, root-mean-square deviation; GRH, growth hormone.

0006-2960/91/0430-11029$02.50/0

1990), and a 3D HSQC–NOESY–HSQC experiment to identify NH–NH NOE connectivities between overlapping amide protons (Frenkiel et al., 1990; Ikura et al., 1990). Full details are given in the supplementary material. The data were processed on a Sun Sparcstation 1 using the FELIX software package (Hare Research Inc.). The $^3J_{HN\alpha}$ coupling constants were obtained from a 2D ^1H–^{15}N HMQC experiment which contained a final $\pi/2(y)$ ^1H pulse (HMQC–*J*) (Kay & Bax, 1990). The coupling constant values were extracted from individual cross sections using spectral simulations; details of the procedures are given as supplementary material. Coupling constants, or upper limits to the coupling constants, were obtained for 111 of the 130 residues in the recombinant IL-4. Amide-exchange rates were estimated using data from 2D ^1H–^{15}N HSQC experiments.

Structure Calculations. Structures were calculated using a hybrid "distance geometry–simulated annealing" protocol (Nilges et al., 1988). A distance geometry (Havel & Wüthrich, 1984) program from Dr. R. Scheek, Groningen, and the program XPLOR (Brünger, 1988) were used; further details of the specific procedure adopted here have been described previously (Sutcliffe & Dobson, 1991). Calculations were run on a Convex C210 minisupercomputer, and the calculation of each structure required ~5 h of CPU time.

Results

Assignment of the NMR Spectrum. The assignment of the majority of ^{15}N and ^1H resonances in the spectrum of IL-4 was achieved using the information contained in two 3D data sets, a NOESY–HMQC collected with a mixing time of 200 ms and a HOHAHA–HSQC collected with an isotropic mixing time of 26 ms. The HOHAHA–HSQC spectrum permitted the correlation of the amide ^{15}N and ^1H chemical shifts with the C^α ^1H shift for 124 of the 130 residues of recombinant IL-4. As a result of the short isotropic mixing period used, and of the large number of small NH–C^αH coupling constants expected for a largely helical protein, only a small number of NH–C^βH peaks were observed in the HOHAHA–HSQC spectrum. Additional spin system information for aromatics and methyl-containing residues was therefore obtained from an analysis of 2D COSY, RELAY, double-RELAY, and NOESY spectra of the unlabeled protein. Using these spectra in conjunction with the 3D NOESY–HMQC and 3D HOHAHA–HSQC spectra, spin system information was identified for 32 residues of the protein. This was sufficient to permit the sequential assignment of the entire spectrum.

The majority of strong sequential NOE's observed for IL-4 were NH–NH, rather than C^αH–NH, as would be expected for a helical protein. The sequential assignment was achieved by identifying stretches of spin systems connected by NOE effects. Assignment of these segments to specific residues in the protein was achieved first for the longest segments which contained amides for which some spin system information was available. Breaks in the sequential assignment occurred, in the majority of cases, because an NH–NH NOE could not be observed for a pair of amides with very similar NH shifts. These connectivities were later identified in a 3D HSQC–NOESY–HSQC spectrum of IL-4, and this confirmed that the assignments based on the shorter segments were correct.

An example of the sequential assignment is illustrated in Figure 1 for residues 74–82. Assignment for the main-chain resonances of 127 of the 130 residues and for approximately 70% of the side-chain protons was achieved for recombinant IL-4 in this work. A complete list of these assignments is given as supplementary material, and the ^{15}N–^1H cross peaks in the HMQC–*J* spectrum are labeled with their assignments in Figure 2.

Secondary Structure Identification. The spectra of the protein were analyzed further to give information about the secondary structure of the protein (Wüthrich, 1986); NOESY cross peaks typical of regular secondary structure units were identified (see Figure 1), $^3J_{HN\alpha}$ values were measured, and the rates of exchange of amide protons (giving information about hydrogen bonds) were categorized. These data for IL-4 are summarized in Figure 3. The strong sequential NH–NH NOE's, the observation of NH–NH(*i*,*i*+2), C^αH–NH(*i*,*i*+2), C^αH–NH(*i*,*i*+3), and C^αH–NH(*i*,*i*+4) NOE's, and the small $^3J_{HN\alpha}$ values for residues in the ranges 5–17 (A), 41–57 (B), 72–90 (C), and 110–125 (D) indicate clearly that these residues adopt helical conformations. In addition, the NOE data show that there is a short region of β-sheet connecting residues 29–31 to residues 106–108. Consistent with these findings is the observation that almost all the slowly exchanging amide protons are found in these regions; slowly exchanging amides are very frequently, although not exclusively, indicative of persistent secondary structure. For three of the helical regions, A, C, and D, the pattern of NOE's characteristic of helices is particularly complete. In the fourth helix, B, although numerous NOE's characteristic of helical structure are observed, there is a missing assignment for residue 53, which is close to the center of the helical region. The hydrogen-exchange data and the observation of a 52C^αH–55NH NOE of medium intensity suggest that the helix is continuous, but the possibility of some irregularity in its structure cannot, at this stage, be eliminated.

Outline Structure for IL-4. More detailed analysis of the 2D and 3D NOESY spectra enabled a total of 1360 NOE's to be identified, including 123 which are longer range (involving residues more than five removed in the sequence) and so define tertiary contacts in the folded protein. Identification of further NOE's could not be achieved reliably because of ambiguities arising from overlap in often poorly dispersed spectral regions. The data are summarized in the diagonal plot in Figure 4 which reveals, in a remarkably direct manner, some notable features of the protein structure. Almost all the long-range data points are concentrated around two lines: a strong "antidiagonal" and a line approximately parallel to this starting around residue 95. The antidiagonal shows that the polypeptide chain must loop back on itself, bringing the N- and C-termini of the protein into close proximity and bringing helices A and D and helices B and C close to each other. In each of these pairs of helical contacts, the chains must run in opposite directions in the two helices. The polypeptide chain also loops round again, as indicated by the other line of points parallel to the antidiagonal, so that residues 1–30 run along side residues 95–55. This means that helix A is also adjacent to helix C and the AB loop is close to the end of helix B. It is interesting that the points for the three disulfide bridges in IL-4, also shown in Figure 4, lie within the two lines of NOE data points. These disulfide bridges link one end of helices A and D together (3–127), the CD loop to helix B (46–99) and the AB loop to the BC loop (24–65).

Preliminary calculations to investigate the more detailed packing of the four helices in IL-4 have been carried out. When calculations were run using only the restraints that are conventionally derived from the experimental NMR data (1360 NOE distance restraints, 99 ϕ angle restraints, and 27 pairs of hydrogen bond distance restraints; details of the restraints used are given in the supplementary material), structures were routinely generated with irregularities in one

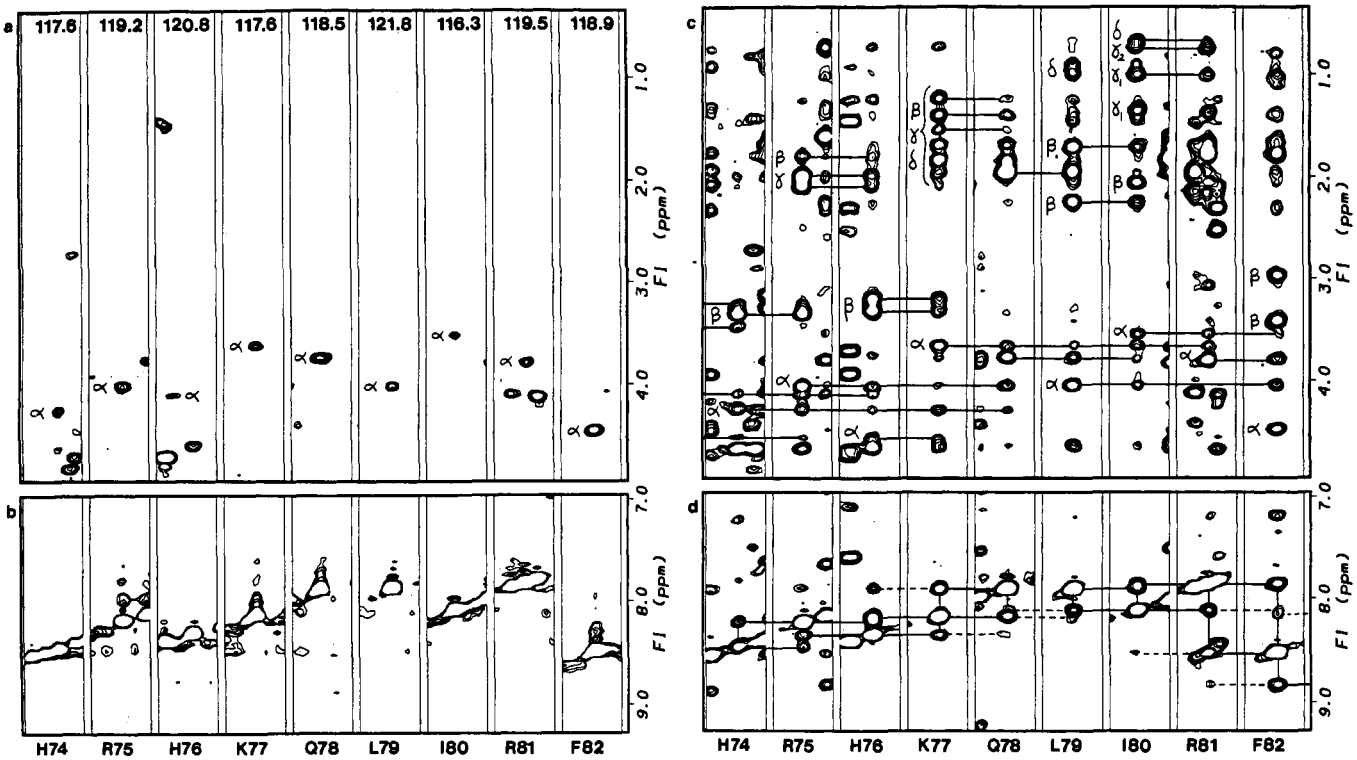

FIGURE 1: (a, b) Composite of amide strips taken from the 3D HOHAHA-HSQC spectrum of IL-4. The NH-C$^{\alpha}$H peak positions for residues H74-F82 are labeled in (a). The numbers at the top of each strip give the $F2$ chemical shift values at which the strips are taken. The NH diagonal peaks are shown in (b). (c, d) Corresponding strips for the 3D NOESY-HMQC spectrum. NH-NH sequential connectivities which can be seen for residues 74-78 and 79-82 are indicated by solid lines. The NOE between residues 78 and 79 is not observed in the 3D NOESY-HMQC spectrum because of chemical shift degeneracy of the two NH resonances. This sequential NOE effect is observed, however, in the 3D HSQC-NOESY-HSQC spectrum as each has different ^{15}N shifts. The resonance assignments based on NH-NH(i,i+1) connectivities are all confirmed by the C$^{\alpha}$H-NH(i,i+1) NOE effects observed in (c). This also shows some of the intra- and interresidue NOE effects between NH and side-chain protons useful for spin system identification. For example, the strong pair of NOE effects between the NH of His 76 and protons at 3.32 and 3.20 ppm is consistent with the assignment of this NH to an AMX spin system such as histidine. Inspection of (c) and (d) also shows a large number NH-NH(i,i+2), C$^{\alpha}$H-NH(i,i+2), C$^{\alpha}$H-NH(i,i+3), and C$^{\alpha}$H-NH(i,i+4) peaks indicated by horizontal lines. These NOE effects permit an identification of secondary structure to be made but also are useful in confirming the sequential assignments.

or more of the helices which gave rise to localized and inconsistent violations of the experimental restraints. Calculations were therefore also run where dihedral angle ϕ and ψ restraints were used, in conjunction with NOE restraints, to restrain the four regions, 5-17, 41-57, 72-90, and 110-125, into more regular helical secondary structures (restraints: $\phi = -60 \pm 5°, \psi = -50 \pm 5°$). Structures calculated in this way had no significant or systematic violations of the experimental data; typically, no more than 10 of the 1360 NOE's were violated by more than 0.5 Å, and all violations were less than 1.3 Å. From a set of 20 structures calculated with these additional ϕ and ψ restraints, the 10 lowest energy structure had a C$^{\alpha}$ RMSD from the average structure of 3.2 Å (for just the helical regions, the value reduces to 2.7 Å). Although there are variations between the calculated structures, all structures of low energy defined by both the methods adopt a "four-helix bundle" type structure. The four-helix bundle is a structural motif found in a range of globular proteins (Presnell & Cohen, 1989) [e.g., cytochrome b-562 (Lederer et al., 1981), myohemerythrin (Hendrickson & Ward, 1977), growth hormone (GRH) (Abdel-Meguid et al., 1987), and interleukin 2 (Brandhuber et al., 1987)]. A schematic representation of the topology of IL-4 found in all the calculated structures is given in Figure 5. This shows that the structure has an up-up-down-down connectivity pattern for the four helices and indicates the position of the disulfide bonds and β-sheet relative to them. The present set of NOE's does not, however, define well the packing of these helices; this is indicated clearly in Figure 6, which shows a representative selection of the structures calculated for IL-4. The orientation of helix D, in particular, varies substantially among the set of calculated structures, and while the packing together of the other three helices is better defined, significant variability in their orientations remains. It is perhaps surprising at first sight that the data set of 1360 NOE's is not sufficient to define the structure more fully; for hen lysozyme, for example, a protein with an identical number of residues, a total of 1158 NOE restraints gives a C$^{\alpha}$ RMSD of the calculated structures from the average of 1.8 ± 0.2 Å for all residues and of 1.2 ± 0.3 Å for the major regions of secondary structure (L. J. Smith, M. J. Sutcliffe, C. Redfield, and C. M. Dobson, unpublished results). A more detailed examination of the present set of NOE's explains, however, at least some of the variations between the various calculated structures of IL-4. For example, NOE effects have been observed, as shown in Figure 4, between the pairs of helices A and B, A and D, and B and C. NOE's between helix B and helix D are only observed, however, from residues at the C-terminus of the former and the N-terminus of the latter. Whether this is simply due to the lack of resolved NOE's at this stage or if it indicates the absence of close contacts is not yet known. The result is that helix D is linked by few restraints to other regions of the molecule and hence cannot be well-defined in the calculated structures. Some other features of the packing, however, appear significant even at this present level of the structural analysis. Thus, the NOE's between helix A and helix C indicate that the C-terminal region of helix C is in close contact with the central region of helix A. This results in the N-terminal region of helix C projecting away from the helical contacts; the disulfide bond between the AB and CD loops may well be important in maintaining the

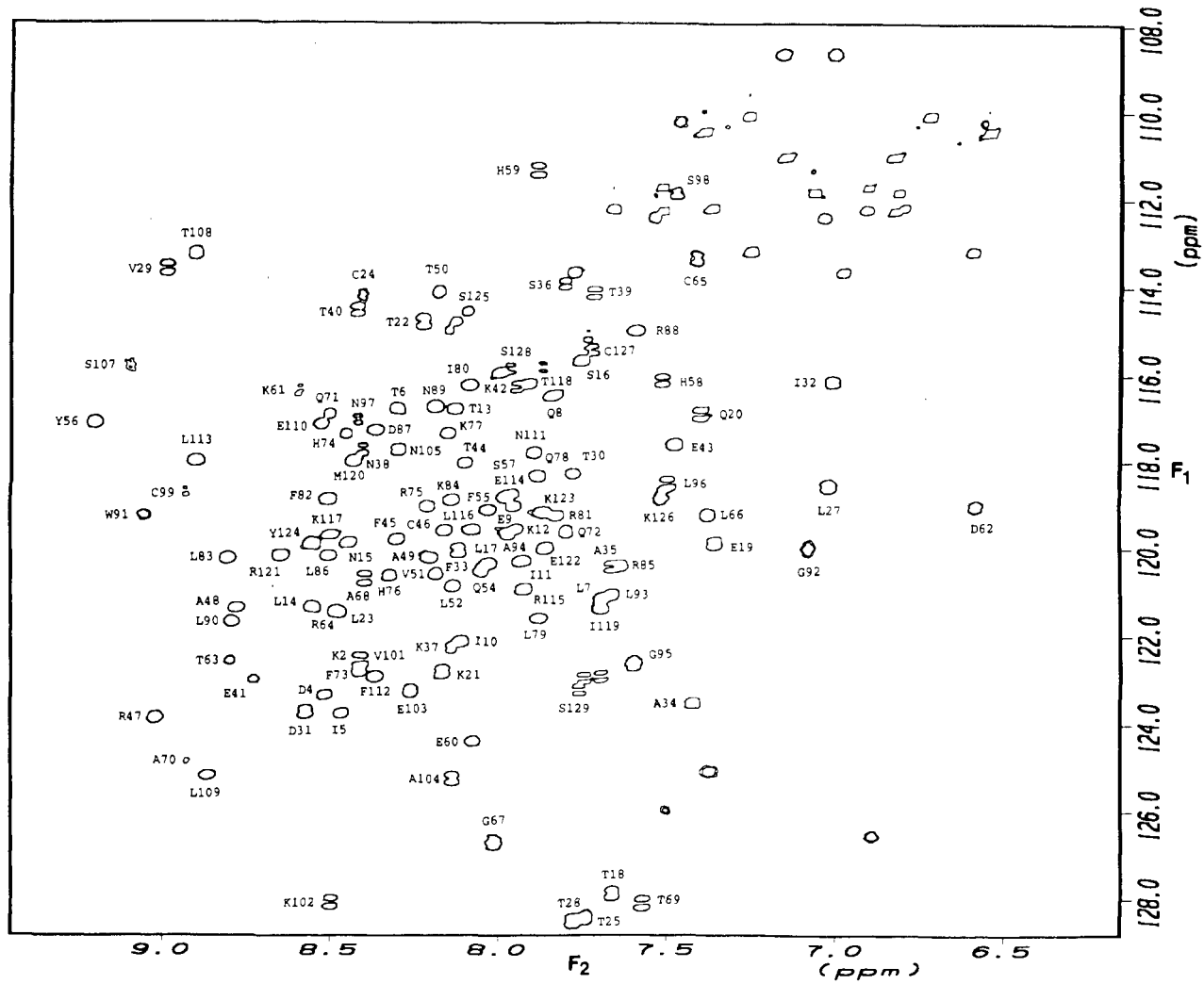

FIGURE 2: ^{15}N–^{1}H HMQC–*J*-correlation spectrum of ^{15}N-labeled IL-4 recorded at pH 5.3 and 35 °C. The peaks of T18, T25, T28, G67, T69, G92, and G95 have been folded in the *F*1 dimension in order to improve the digital resolution; the correct ^{15}N shifts for these resonances are listed in the supplementary material. The data have been resolution enhanced with a phase-shifted sine bell in *F*1 in order to improve the resolution of individual cross peaks in the spectrum. Cross peaks which display doublet fine structure in *F*1 correspond to residues with a large NH–C$^{\alpha}$H coupling constant (i.e., T39 and A104).

packing in this region of the structure. Furthermore, the connectivity of the molecule found here means that the AB and CD loops run the length of the molecule. Although discussion of details of the topology of these is premature, it is interesting that both these loops not only are cross-linked by disulfide bonds to other regions of the molecule but are linked to each other by the short region of β-sheet structure. These considerations, along with the significant number of NOE's observed already to involve these loops, suggest that they are likely to be rather well ordered in the structure.

Discussion

The majority of the structures which adopt the four-helix bundle motif have an up–down–up–down connectivity with short loops connecting the helices (Presnell & Cohen, 1989). The up–up–down–down connectivity found here for IL-4 is therefore different from these. This type of structure has, however, been found previously for the GRH molecule, although there are distinctive features in the IL-4 molecule. In particular, IL-4 has three disulfide bonds compared to two in GRH, and the region of β-sheet in IL-4 appears to have no precedent. We suggest that these additional cross-linkages in IL-4 are needed as a result of its smaller size; IL-4 has only 129 residues compared with the 191 residues of porcine GRH. The shorter helices and consequently reduced helix–helix contacts of IL-4 may be compensated for by the stabilizing effects of these additional interactions.

Of particular interest in the light of the present structural conclusions is a comparison of the human IL-4 sequence with that of the mouse protein (DeFrance et al., 1987a; Carr et al., 1991). In the latter protein, sequence alignments indicate the absence of the 3–127 disulfide bond and its replacement with a disulfide bond linking residues 3 and 92 (human sequence numbers). The other two disulfide bonds remain similar in the two molecules. The structure of IL-4 described here would enable this sequence change to be accommodated readily; the change in disulfide linkages means that instead of the structure having a bond between the N-terminus of helix A and the C-terminus of helix D, it is between the N-terminus of helix A and the C-terminus of helix C. This would need little structural rearrangement provided that the C-terminus of helix C is near to the N-terminus of helix A in the structure of the protein; this proximity is in fact defined by a number of crucial NOE's between residues 6 and 93 in the human protein. It is interesting to note that if the disulfide connectivity found in the mouse protein were to be positioned on the diagonal plot of Figure 4, it too would lie within the line of data points parallel to the main antidiagonal discussed earlier. The other changes from the human to the mouse protein involve deletion of four C-terminal residues and extension of the N-terminus

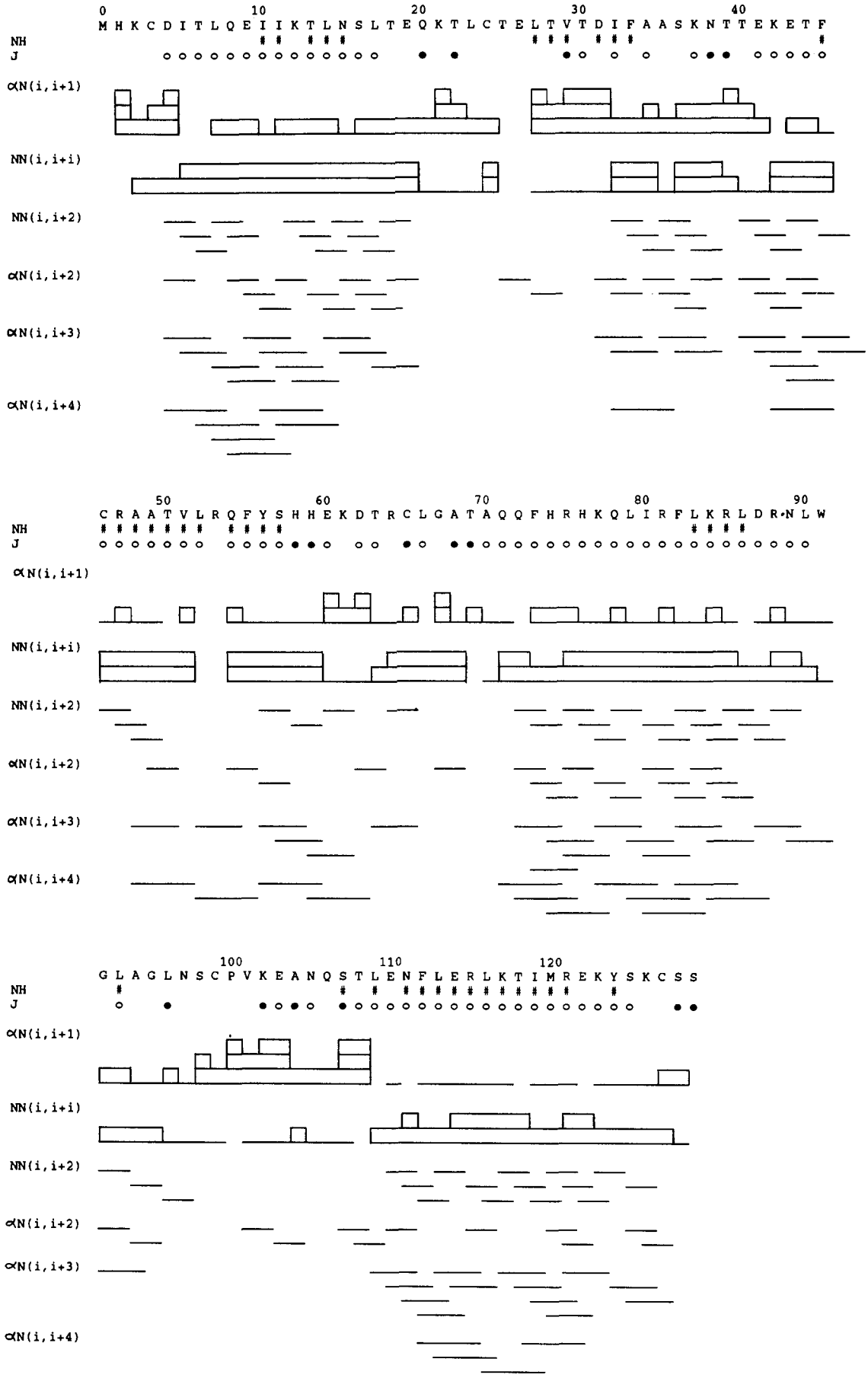

FIGURE 3: Sequence of human IL-4 together with a summary of the NMR data defining the secondary structure of the protein. For the short-range NOE's involving NH and $C^{\alpha}H$ protons, the NOE intensities are indicated by the width of the bars. Residues with amide NH resonances that are slow to exchange (i.e., those that are not fully exchanged 1 h after the protein is dissolved in D_2O at pH 4.5 and 20 °C) are shown by #. Residues with $^3J_{HN\alpha}$ <6 Hz are indicated by open circles and those with $^3J_{HN\alpha}$ >8 Hz by solid circles.

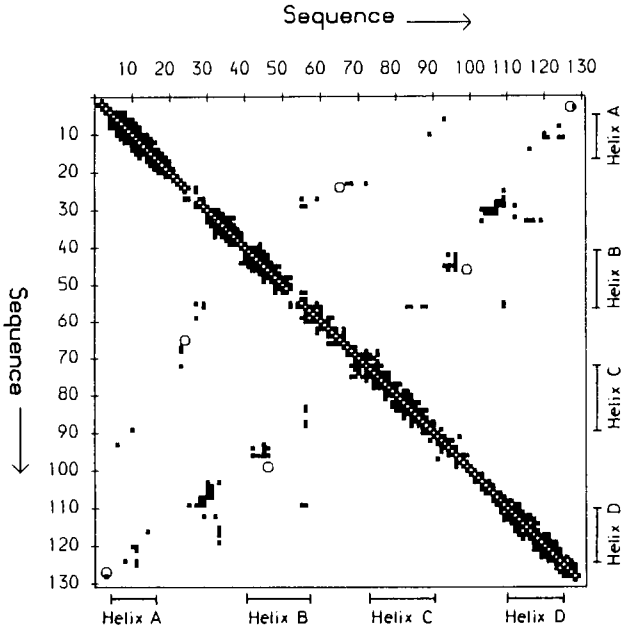

FIGURE 4: Plot showing pairs of amino acid residues for which an NOE effect has been observed. The location of the helices in the structure is indicated along the axes, and the disulfide connectivities are indicated by open circles.

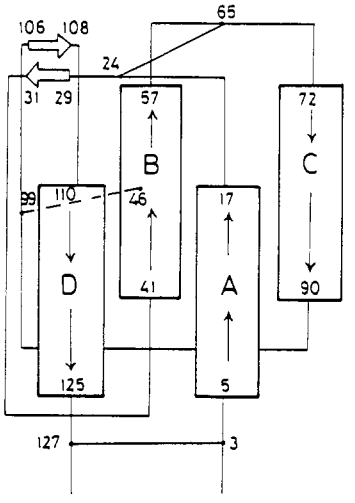

FIGURE 5: Schematic diagram of the main-chain fold of the structures calculated for human IL-4, showing the up–up–down–down connectivity and the positions of the disulfide bridges and the short region of β-sheet.

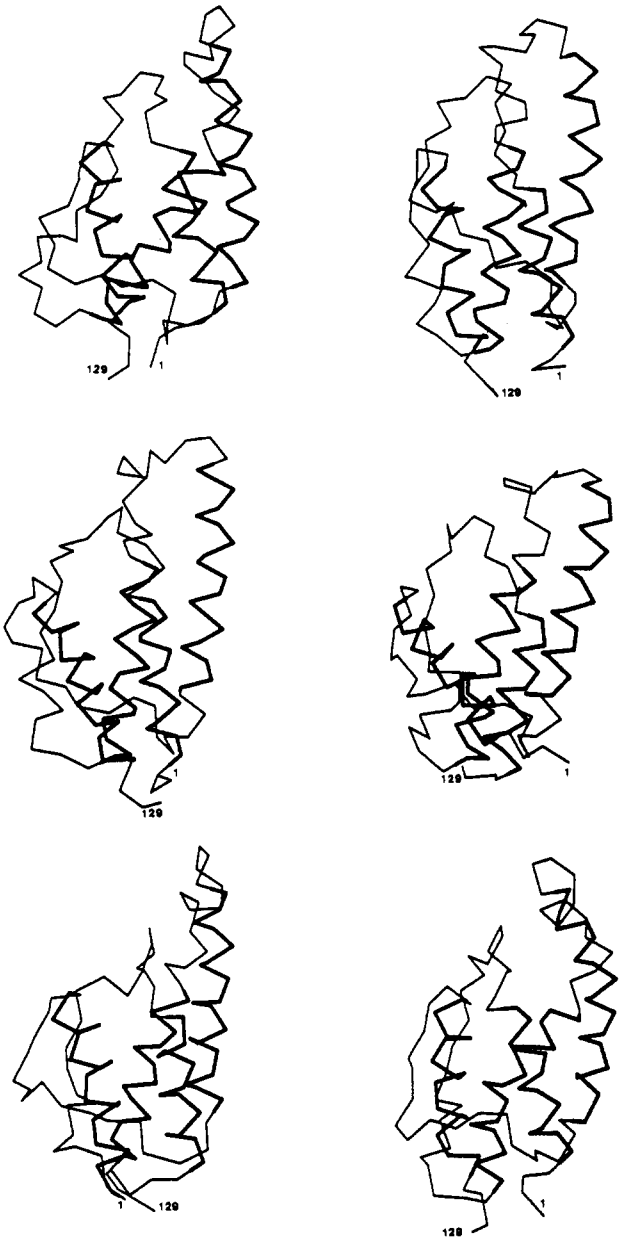

FIGURE 6: Preliminary structures of human IL-4 calculated from the NMR data presented in this paper. Note that the overall topology is relatively well-defined, but there are substantial variations in the details of the structures. In particular, there is a lack of definition for helix D relative to the other three helices, and there are significant differences in the loop conformations.

by six residues and deletion of residues 67–73. The 67–73 residues are in the BC loop which could presumably be shortened without major disruption of the overall packing of the helices themselves.

From the results of the structural analysis described above, it is evident that the NOE data obtained for the ^{15}N-labeled sample are adequate to define the overall fold of IL-4 in solution. Details of the structure, in particular the angles between the helices and the topology where the long AB and CD loops meet, cannot, however, yet be reliably defined. For a helical protein, in contrast to one involving significant regions of β-sheet structure, the contacts between regions of secondary structure distant in the primary sequence almost invariably involve side-chain atoms. In order to define these contacts, it is therefore necessary to assign the majority of the side-chain resonances in the NMR spectrum and to have sufficient resolution to be able to detect NOE's between them. The spectra of uniformly ^{15}N-labeled IL-4 have proved remarkably effective for assignment of the main-chain resonances and for identification of secondary structure, but resolution of side-chain resonances is dependent on the less well resolved 2D experiments. Experiments are therefore in progress involving ^{13}C–^{15}N double-labeled material. With the additional information about side-chain interactions provided by such experiments (Kay et al., 1990), refinement of the present structure to a substantially higher level of detail should be possible.

The outline structure of human IL-4 described in this paper is of particular importance for two reasons. First, it provides experimental support for the hypothesis that many helical cytokines may have a common tertiary fold, despite a lack of significant sequence homology; the structure type found previously for GRH, and now for IL-4, has in fact been predicted for IL-4 itself (Idzerda et al., 1990) and also for erythropoietin (EPO), interleukin 6, and granulocyte colony-stimulating

factor (G-CSF), (Bazan, 1990b). Second, it provides the opportunity to test the hypothesis that hemopoietic cytokines react with their receptors via a two-step mechanism involving a helical region common to different cytokines and a more specific secondary interaction (Bazan, 1990a,b). Particularly interesting in this regard are the projected differences between the mouse and human IL-4 structures, as these proteins do not cross-react with each other's receptors. The level of structural detail now available for IL-4 is sufficient to allow mutagenesis of helical and loop regions to be carried out, in a systematic manner, to probe its biological functions.

Acknowledgments

We thank the following at SmithKline Beecham for their assistance in the production and characterization of IL-4: C. Gershater, I. Dodd, C. Entwisle, H. Edwards, J. Edwards, and V. Spackman. We gratefully acknowledge B. Weston, S. Box, M. J. Browne, J. M. Dewdney, and D. V. Gardner for support and encouragement. We thank Paul Driscoll for his help with the processing and display of the 3D data and with the measurement of NH–$C^{\alpha}H$ coupling constants. We also thank Nick Soffe for his assistance with the implementation of the 3D experiments.

Supplementary Material Available

A listing of the assignments for IL-4 together with further details of the experimental NMR procedures (10 pages). Ordering information is given on any current masthead page.

References

Abdel-Meguid, S. S., Shiel, H.-S., Smith, W. W., Dayringer, H. E., Violand, B. N., & Bentle, L. A. (1987) *Proc. Natl. Acad. Sci. U.S.A. 84*, 6434–6437.

Bazan, J. F. (1990a) *Proc. Natl. Acad. Sci. U.S.A. 87*, 6934–6938.

Bazan, J. F. (1990b) *Immunol. Today 11*, 350–354.

Brandhuber, B. J., Boone, T., Kenney, W. C., & McKay, D. B. (1987) *Science 238*, 1707–1709.

Brünger, A. T. (1988) *XPLOR Manual*, Yale University, New Haven, CT.

Carr, C., Aykent, S., Kimack, N. M., & Levine, A. D. (1991) *Biochemistry 30*, 1515–1523.

Clore, G. M., & Gronenborn, A. M. (1991) *Science 253*, 1390–1399.

Cook, W. J., Ealick, S. E., Reichert, P., Hammond, G. S., Le, H. V., Nagabhushan, T. L., Trotta, P. P., & Bugg, C. E. (1991) *J. Mol. Biol. 218*, 675–678.

DeFrance, T., Vanbervliet, B., Aubrey, J. P., Takebe, Y., Arai, N., Miyajima, A., Yokota, T., Lee, F., Arai, K., de Vries, J. E., & Banchereau, J. (1987a) *J. Immunol. 139*, 1135–1141.

DeFrance, T., Aubrey, J. P., Rousset, F., Vanbervliet, B., Bonnefoy, J. Y., Arai, N., Takebe, Y., Yokotai, T., Lee, F., de Vries, J., & Banchereau, J. (1987b) *J. Exp. Med. 165*, 1459–1467.

Driscoll, P. C., Clore, G. M., Marion, D., Wingfield, P. T., & Gronenborn, A. M. (1990) *Biochemistry 29*, 3542–3556.

Frenkiel, T., Bauer, C., Carr, M. D., Birdsall, B., & Feeney, J. (1990) *J. Magn. Reson. 90*, 420–425.

Havel, T., & Wüthrich, K. (1984) *Bull. Math. Biol. 46*, 673–698.

Hendrickson, W. A., & Ward, K. B. (1977) *J. Biol. Chem. 252*, 3012–3018.

Howard, M., Farrar, J., Hilfiker, M., Johnson, B., Takatsu, K., Hamaoka, T., & Paul, W. E. (1982) *J. Exp. Med. 155*, 914–923.

Idzerda, R. L., March, F. J., Mosley, B., Lyman, S. D., Vanden Bos, T., Gimpel, S. D., Din, W. S., Grastein, K. H., Widmer, M. D., Park, L. S., Cosman, D., & Beckmann, M. P. (1990) *J. Exp. Med. 171*, 861–873.

Ikura, M., Bax, A., Clore, G. M., & Gronenborn, A. M. (1990) *J. Am. Chem. Soc. 112*, 9020–9022.

Kawakami, Y., Rosenberg, S. A., & Lotze, M. T. (1988) *J. Exp. Med. 168*, 2183–2191.

Kay, L. E., & Bax, A. (1990) *J. Magn. Reson. 86*, 110–126.

Kay, L. E., Clore, G. M., & Gronenborn, A. M. (1990) *Science 249*, 411–414.

Lederer, F., Glatigny, A., Bethge, P. H., Bellamy, H. D., & Mathews, F. S. (1981) *J. Mol. Biol. 148*, 427–448.

Marion, D., Driscoll, P. C., Kay, L. E., Wingfield, P. T., Bax, A., Gronenborn, A. M., & Clore, G. M. (1989) *Biochemistry 28*, 6150–6156.

Messerle, B. A., Wider, G., Otting, G., Weber, C., & Wüthrich, K. (1989) *J. Magn. Reson. 85*, 608–613.

Nilges, M., Clore, G. M., & Gronenborn, A. M. (1988) *FEBS Lett. 229*, 317–324.

Presnell, S. R., & Cohen, F. E. (1989) *Proc. Natl. Acad. Sci. U.S.A. 86*, 6592–6596.

Redfield, C., & Dobson, C. M. (1988) *Biochemistry 27*, 122–136.

Sutcliffe, M. J., & Dobson, C. M. (1991) *Proteins 10*, 117–129.

van Kimmenade, A., Bond, M. W., Schumacher, J. H., Laquoi, C., & Kastelein, R. A. (1988) *Eur. J. Biochem. 173*, 109–114.

Vercelli, D., Jabara, H. H., Arai, K.-I., & Geha, R. S. (1989) *J. Exp. Med. 169*, 1295–1307.

Windsor, W. T., Syto, R., Le, H. V., & Trotta, P. P. (1991) *Biochemistry 30*, 1259–1264.

Wüthrich, K. (1986) *NMR of Proteins and Nucleic Acids*, Wiley, New York.

Wüthrich, K. (1989) *Acc. Chem. Res. 22*, 36–44.